

## Cross-correlation between a carbonyl C' chemical shift anisotropy and a long-range dipolar C'HA coupling in proteins using symmetrical reconversion

Karine Loth, Philippe Pelulessy\* & Geoffrey Bodenhausen

*Département de Chimie, associé au CNRS, Ecole Normale Supérieure, 24 rue Lhomond, 75231 Paris cedex 05, France*

Received 11 March 2003; Accepted 2 May 2003

*Key words:* chemical shift anisotropy, dipole-dipole interactions, NMR cross-correlation rates, protein dynamics, protein structure

### Abstract

A new sequence is described to measure the cross-correlation rates between the chemical shift anisotropy of the carbonyl carbon-13 nucleus and the dipole-dipole interaction between this carbonyl and the alpha-proton in proteins. The sequence is based on the symmetrical reconversion principle and is insensitive to experimental errors and to violations of the secular approximation. The cross-correlation rate depends on the backbone angle  $\psi$ . The advantages and limitations of the sequence are discussed.

*Abbreviations:* CSA – chemical shift anisotropy; DD – dipole-dipole; MQC – multiple quantum coherence; NMR – nuclear magnetic resonance; SQC – single quantum coherence.

### Introduction

Cross-correlated relaxation rates depend on the angle subtended between two tensorial interactions, thus providing valuable structural information (Reif et al., 1997; Schwalbe, 2001; Kloiber et al., 2002). For example, the cross-correlation rate between the two dipole-dipole (DD) interactions  $NH^N$  and  $H^N H^\alpha$  in proteins depends on  $\phi$ -angles (Boyd et al., 1991). In spectra of single quantum coherences (SQC), cross-correlated relaxation rates cause lines that correspond to different single-transition operators to relax differentially (Goldman, 1984). The frequencies of the single-transition operators are separated by scalar couplings. Whenever these scalar couplings become small, overlap of resonances makes it difficult to extract accurate line widths, and their shapes can be affected by transverse cross-relaxation due to the violation of the secular approximation (Palmer et al.,

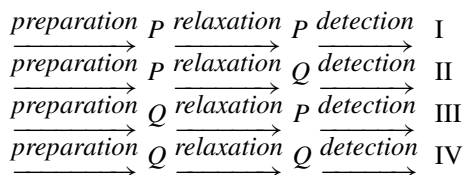
1992). The measurement of cross-correlated relaxation rates of SQC's in macromolecules have therefore been mainly limited to interference effects between a chemical shift anisotropy (CSA) and a DD interaction with a directly attached nucleus. Cross-correlation rates can also be measured in a time-domain approach by monitoring the build-up of an operator  $Q$  that results from partial conversion of an initial operator  $P$  (Tjandra et al., 1996). The expectation values of the operators evolve as

$$\frac{\langle Q \rangle (t)}{\langle P \rangle (t)} = \tanh (R_{CC} t) . \quad (1)$$

Measurement of both expectation values  $\langle Q \rangle$  and  $\langle P \rangle$  as a function of time allows one to circumvent problems due to overlap, but does not resolve problems due to violations of the secular approximation. Furthermore, errors might be introduced if the operators  $Q$  and  $P$  cannot be detected with the same efficiency. We have recently introduced a new scheme based on the time-domain approach that greatly alleviates both problems (Pelupessy et al., 2003). The

\*To whom correspondence should be addressed. E-mail: Philippe.Pelulessy@ens.fr

approach is based on detecting the decay of *both* operators  $Q$  and  $P$ , and monitoring the conversion of  $Q$  into  $P$  and *vice-versa*. The scheme can be summarised as follows



From these four experiments, which we named *symmetrical reconversion* scheme, the cross-correlation rate can be easily extracted :

$$\sqrt{\frac{\langle Q \rangle_{\text{II}}(t) \langle P \rangle_{\text{III}}(t)}{\langle P \rangle_{\text{I}}(t) \langle Q \rangle_{\text{IV}}(t)}} = \tanh(|R_{CC}|t). \quad (2)$$

Since the same detection and preparation blocks are used in the experiments that contribute to the denominator of Equation 2 as in the experiments that determine the numerator, errors due to unequal detection efficiencies are automatically cancelled. Moreover, this scheme is much less sensitive to violations of the secular approximation, as can be demonstrated by simulation. In this article we present a new scheme based on the symmetrical reconversion principle to measure the cross-correlated relaxation rate in proteins due to interference between the CSA of the  $C'$  carbonyl nucleus and the long-range dipole-dipole  $C'H^\alpha$  interaction. This rate is related to the  $\Psi$ -angle.

### Pulse sequence and theory

Figure 1 shows a few atoms in the vicinity of the  $C'$  carbonyl nucleus in proteins. The cross correlation rate  $R(C'/C'H^\alpha)$  is given by (Goldman, 1984).

$$\begin{aligned}
 R(C'/C'H^\alpha) = & \frac{\mu_0 \hbar \gamma_C^2 \gamma_H B_0}{24 \pi r^3(C'H^\alpha)} \{ (\sigma_{xx} - \sigma_{zz}) \\
 & [4J_{xx,CH}(0) + 3J_{xx,CH}(\omega_C)] + \\
 & (\sigma_{yy} - \sigma_{zz}) [4J_{yy,CH}(0) \\
 & + 3J_{yy,CH}(\omega_C)] \}, \quad (3)
 \end{aligned}$$

where  $\sigma_{ii}$  are the principal components of the  $C'$  CSA tensor as depicted in Figure 1,  $\mathbf{r}(C'H^\alpha)$  is the distance between the  $C'$  and  $H^\alpha$  nuclei and the other symbols have their usual meaning. In the absence of fast local motions the spectral density  $J(\omega)$  is given by

$$J_{ii,CH}(\omega) = \frac{2}{5} P_2 \cos(\Theta_{ii,CH}) \frac{\tau_c}{1 + \omega^2 \tau_c^2}, \quad (4)$$

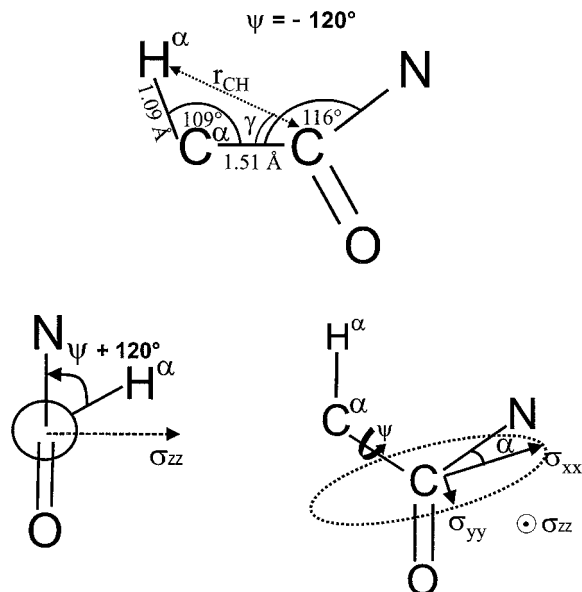


Figure 1. Atoms in the vicinity of the carbonyl carbon  $C'$  in proteins. The dihedral angle  $\psi$  around the  $C'C^\alpha$ -bond is indicated on the Newman projection. The principal components of the CSA tensor  $\sigma_{xx}$ ,  $\sigma_{yy}$  and  $\sigma_{zz}$  are oriented so that the most shielded component  $\sigma_{zz}$  is perpendicular to the peptide plane, while the least shielded component  $\sigma_{xx}$  subtends an angle  $\alpha$  with respect to the  $C'N$  bond. All atoms shown lie in the same plane if  $\psi = -120^\circ$ .

where  $\Theta_{ii,CH}$  is the angle between the  $\sigma_{ii}$  component and the vector  $\mathbf{r}(C'H^\alpha)$ . Using the standard geometry of Figure 1 these angles can be expressed as:

$$\cos \Theta_{xx,CH} = -\cos(\gamma) \cos(64^\circ - \alpha) + \sin(\gamma) \sin(64^\circ - \alpha) \cos(\psi - 120^\circ) \quad (5a)$$

$$\cos \Theta_{yy,CH} = -\cos(\gamma) \cos(154^\circ - \alpha) + \sin(\gamma) \sin(154^\circ - \alpha) \cos(\psi - 120^\circ), \quad (5b)$$

where  $\alpha$  is the angle between  $\sigma_{xx}$  and the vector  $\mathbf{r}(C'N)$  and  $\gamma$  the angle between the vectors  $\mathbf{r}(C'H^\alpha)$  and  $\mathbf{r}(C'C^\alpha)$ .

The sequence used to measure the CSA/DD cross-correlation rate  $R(C'/C'H^\alpha)$  is shown in Figure 2. At point  $b$  in the sequence the operator  $2C'_z N_z$  is created. For experiments **I** and **II** the relaxation period  $T$  starts after a  $(\pi/2)_x$  pulse is applied to the protons in order to destroy any spurious  $4H_z^\alpha C'_z N_z$  coherence. A  $(\pi/2)_x$  pulse is applied to  $C'$  to create a  $-2C'_y N_z$  coherence. In experiments **III** and **IV** three successive INEPT steps create three spin order  $4H_z^\alpha C'_z N_z$ . Two proton  $\pi/2$  pulses, of which the second one is phase-alternated, are followed by a  $\pi/2$  pulse applied to  $C'$  to select the  $-4H_z^\alpha C'_y N_z$  coherence. During the relaxation period  $T$ ,  $C'^\alpha$ -decoupling is applied to suppress

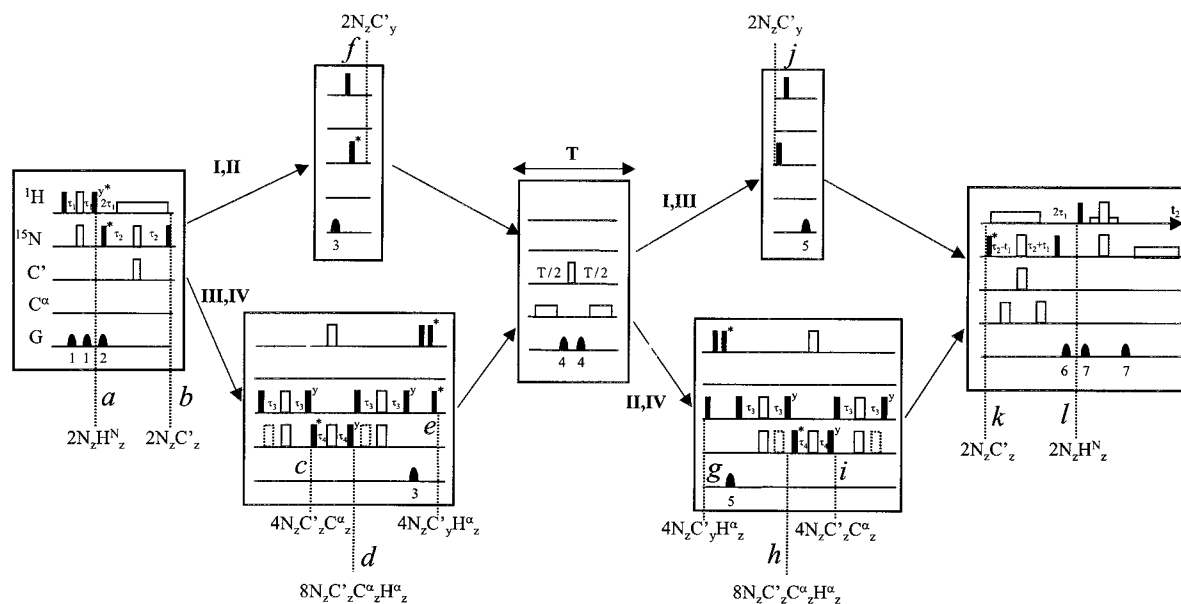


**Figure 2.** Symmetrical reconversion sequences used to measure the cross-correlation rate  $R(C'/C'H^\alpha)$ . A set of four experiments is performed. In experiments **I** and **II** the operator  $2C'_y N_z$  is created while in experiments **III** and **IV** one excites  $4H_z^\alpha C'_y N_z$ . After the relaxation period  $T$ , the  $2C'_y N_z$  coherence is detected in experiments **I** and **III** while  $4H_z^\alpha C'_y N_z$  is selected and converted into  $2C'_y N_z$  in experiments **II** and **IV**. In all four experiments the  $2C'_y N_z$  order is converted into detectable  $H_x^N$  coherence after  $t_1$  evolution of the amide nitrogen. Filled and open rectangles correspond to  $\pi/2$  and  $\pi$  pulses. Dotted rectangles stand for  $\pi$  pulses that compensate for Bloch-Siegert shifts. Long open rectangles represent decoupling. Short low rectangles stand for selective  $\pi/2$  pulses applied at the water resonance. All phases are along the  $x$ -axes unless specified otherwise. The phases of  $\pi/2$  pulses marked by asterisks are alternated independently while the signals are added and subtracted. The delays are set to  $\tau_1 = 1/4^1 J(\text{NH}^N) = 2.7$  ms,  $\tau_2 = 1/4^1 J(\text{NC}') = 16.5$  ms,  $\tau_3 = 1/4^1 J(\text{C}'\text{C}^\alpha) = 4.5$  ms and  $\tau_4 = 1/4^1 J(\text{C}^\alpha\text{H}^\alpha) = 1.7$  ms.

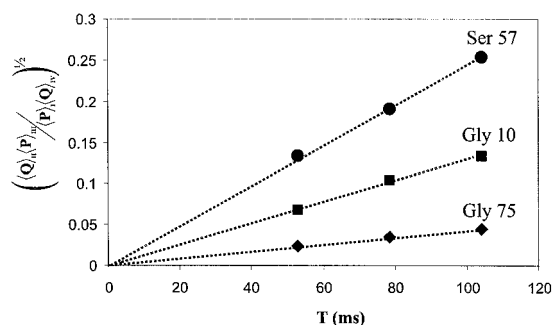


**Figure 3.** Peak heights measured with the sequence of the Figure 2 for three different relaxation delays  $T = 52.9, 78.5$  and  $104.1$  ms. The ratio of Equation 2 is plotted against the relaxation delay  $T$  for three representative residues of human ubiquitin.

effects of the longitudinal  $R(C^\alpha/C^\alpha H^\alpha)$  (CSA/DD) cross-correlation rate (McCoy and Mueller, 1992). In experiments **I** and **III** the  $2C'_y N_z$  coherence is detected after the relaxation period  $T$ . A  $\pi/2$  pulse is applied to the protons, followed by a gradient pulse, in order to suppress spurious  $4H_z^\alpha C'_y N_z$  coherence. In experiments **II** and **IV** the  $4H_z^\alpha C'_y N_z$  coherence is selected and converted into  $2C'_y N_z$ . In all four experiments the

$2C'_y N_z$  coherence is converted into a detectable  $H_x^N$  coherence after a  $t_1$  evolution of the amide nitrogen.

## Results

The cross-correlated relaxation rate  $R(C'/C'H^\alpha)$  has been measured for a sample of  $^{13}\text{C}/^{15}\text{N}$  labelled human ubiquitin (100  $\mu\text{l}$ , 1.5 mM, pH 4.5) at a temperature of 300 K and a proton Larmor frequency of 600 MHz. The 2D spectra were recorded with the scheme of Figure 2, with 56 and 512 complex points in the  $t_1$  and  $t_2$  dimensions and 128 scans per  $t_1$  increment. The carbon carrier frequency was positioned in the center of the carbonyl region (177 ppm), shifted to the center of the carbon- $\alpha$  region (55 ppm) between points  $c$  and  $d$ , and again between points  $h$  and  $i$  of the sequence of Figure 2. The carbon  $\pi/2$  pulses (which must affect either  $C'$  or  $C^\alpha$  regions, without necessarily excluding the  $C^\beta$  region) had square profiles with RF strengths of  $\Delta/\sqrt{15}$ , where  $\Delta$  is the separation between the carbonyl and carbon- $\alpha$  region. The carbon  $\pi$  pulses had G3 profiles and durations of 350  $\mu\text{s}$ . Note that there is no need to refocus the scalar coup-

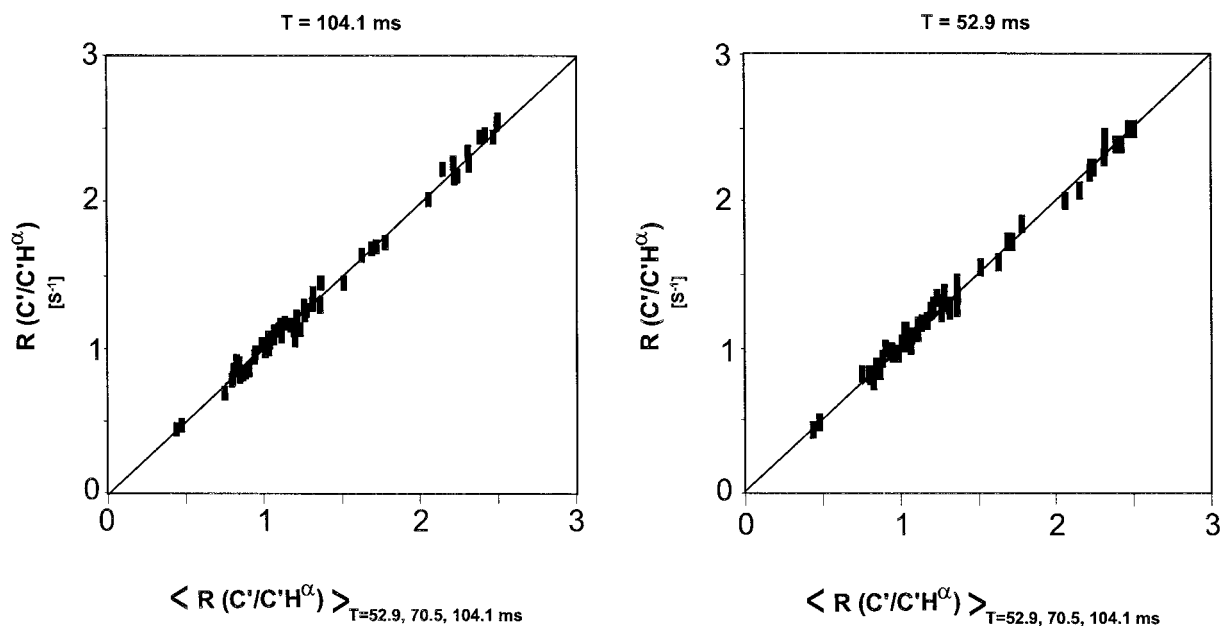


Figure 4. The rates  $R(C'/C'H^\alpha)$  obtained with the shortest and longest  $T$  delays are plotted against the average value of  $R(C'/C'H^\alpha)$ .

lings  $J(C^\alpha C^\beta)$  because of the shortness of the delays  $2\tau_4 = 1/2J(C^\alpha H^\alpha)$  where the  $C^\alpha$ -spins are sensitive to these couplings. Three experiments were performed with relaxation delays  $T = 52.9, 78.5$  and  $104.1$  ms. In Figure 3 the ratio of equation 2 is plotted against  $T$  for three representative residues. In Figure 4 the rates obtained for the shortest and longest relaxation delays  $T$  are plotted against the average rates. The results at different relaxation delays  $T$  agree remarkably well with an error in the average rates of only  $0.04 \text{ s}^{-1}$ .

In Figure 5 the cross-correlation rates thus determined and the theoretical curves derived from Equations 3–5 are plotted against the  $\psi$ -angle. The values for the principal components and the orientations of the CSA tensors are taken from Bax and Cornilescu (2000), who derived the CSA parameters from chemical shift differences of ubiquitin in isotropic and liquid crystalline phases, assuming the orientations and magnitudes of the CSA tensors either to be the same for all residues or only for a subset of amino acids. For curve (a) CSA tensors averaged over all amino acids were used ( $\alpha = 38^\circ$ ,  $\sigma_{xx} = -74.7$ ,  $\sigma_{yy} = -11.8$ ,  $\sigma_{zz} = 86.5$ ), while for curves (b) and (c) distinct CSA tensors were used for  $\beta$ -sheets ( $\alpha = 37^\circ$ ,  $\sigma_{xx} = -76.5$ ,  $\sigma_{yy} = -7.5$ ,  $\sigma_{zz} = 84.0$ ) or for  $\alpha$ -helices ( $\alpha = 42^\circ$ ,  $\sigma_{xx} = -71.2$ ,  $\sigma_{yy} = -23.3$ ,  $\sigma_{zz} = 94.5$ ).

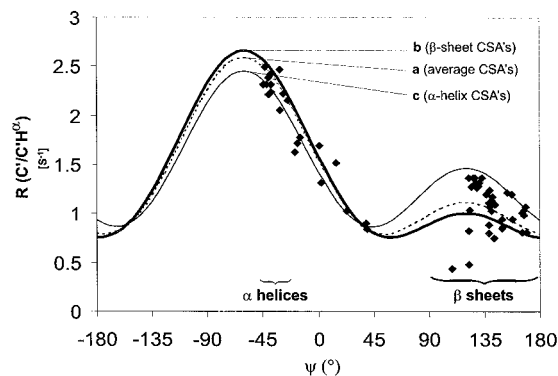


Figure 5. Measured cross-correlation rate plotted against  $\psi$ -angles and theoretical curves derived from equations 3–5. The  $\psi$ -angles were obtained from the NMR structure (Cornilescu et al., 1998). The values for the principal components and the orientations of the CSA tensor are taken from Bax and Cornilescu (2000). The dotted curve is obtained with average CSA values, the thick curve with CSA values derived for  $\beta$ -sheets and the thin curve with CSA values appropriate for  $\alpha$ -helices.

## Discussion

The correlation between the experimental results and curve (a) of Figure 5 is quite reasonable, although one would expect the experimental rates to be lower if one took internal motion into account. Surprisingly the rates calculated for  $\beta$ -sheets seem to fit better with experimental rates for resonances in  $\alpha$ -helices which have negative  $\psi$ -angles and vice-versa. This is exactly

the opposite of what is expected. The reason for this discrepancy probably lies in internal motions. Indeed the cross-correlation rate  $R(C'/C'H^\alpha)$  is affected by an order parameter  $S^2$  while the residual chemical shift is weighted by  $S = \sqrt{S^2}$ , so that the cross-correlation rate is more sensitive to fast internal motions. On the other hand, residual CSA's are more sensitive to slower internal motions. We intend to measure a full set of cross-correlation rates that depend on the CSA of  $C'$  as suggested by Ghose et al. (1998) in order to determine the source of the inconsistencies between the different methods.

It is useful to compare these new experiments with those developed to measure cross-correlation rates of multiple quantum coherences (Reif et al., 1997), in particular with MQC sequences designed to measure the effect on  $C'C^\alpha$ -coherences of the cross-correlation rate  $R(C'/C'H^\alpha)$  (Yang et al. 1997). We have compared the most sensitive version of this MQC experiment (Chiarparin et al. 1999) with our new scheme. At a proton Larmor frequency of 600 MHz (400 MHz),  $R(C'/C'H^\alpha)$  varies from 10 to  $-15$  ( $7$  to  $-10$ )  $s^{-1}$  for a molecule of the size of ubiquitin. This rate amounts to about 60% (40%) of the auto-correlated relaxation rate of the MQC  $2C'_x C_x^\alpha$ , while  $R(C'/C'H^\alpha)$  represents only about 20% (30%) of the relaxation rate of the SQC  $C'_x$ . Hence, specially at higher magnetic fields, the MQC experiments are expected to be more sensitive. However, for  $R(C'/C'H^\alpha)$  there is a clear distinction between conformations with  $\psi$ -angles that are positive and negative. The relaxation period  $T$  is quite simple and does not require any prolonged selective  $C^\alpha$  pulses. Moreover, the sensitivity of the MQC experiments is considerably reduced for residues which have  $C^\beta$  resonances in the  $C^\alpha$  region. The cross-correlation effect that converts MQC  $2C'_x C_x^\alpha$  into  $4C'_y C_y^\alpha H_z^\alpha$  inevitably results from a combination of  $R(C'/C'H^\alpha)$  and  $R(C^\alpha/C'H^\alpha)$ , thus reducing the accuracy. The new SQC experiment is less sensitive to pulse miscalibrations, especially of proton pulses. Pulse miscalibrations diminish the signal-to-noise ratio but hardly contribute to systematic errors in the rates. The rates of the SQC and MQC experiments could be used in a complementary way. If one only has time to perform a single experiment, the new SQC scheme appears to be preferable, provided the signal-to-noise ratio is sufficient.

## Conclusions

A new sequence, based on the principles of symmetrical reconversion, has been presented to measure the cross-correlation rate  $R(C'/C'H^\alpha)$  between the CSA of the carbonyl nucleus  $C'$  and the DD interaction  $C'H^\alpha$  in proteins. The sequence is insensitive to errors due to violations of the secular approximation and automatically compensates for unequal detection efficiencies of various terms in the density operators. The rate  $R(C'/C'H^\alpha)$  provides independent information on dihedral  $\psi$  angles in proteins, although effects of internal dynamics must be taken into account. The rates measured in human ubiquitin show a good correlation with predicted values.

## Acknowledgements

This work was supported by the Centre National de la Recherche Scientifique, the European Union through the Research Training Network 'Cross-Correlation' HPRN-CT-2000-00092 and a fellowship of the Ministère Délégué à la Recherche et aux Nouvelles Technologies to K.L.

## References

- Bax, A. and Cornilescu, G. (2000) *J. Am. Chem. Soc.*, **122**, 10143–10154.
- Boyd, J., Hommel, U. and Krishnan, V.V. (1991) *Chem. Phys. Lett.*, **187**, 317–324.
- Chiarparin, E., Pelupessy, P., Ghose, R. and Bodenhausen, G. (1999) *J. Am. Chem. Soc.*, **121**, 6876–6883.
- Cornilescu, G., Marquardt, J.L., Ottiger, M. and Bax, A. (1998) *J. Am. Chem. Soc.*, **120**, 6836–6837.
- Ghose, R., Huang, K. and Prestegard, J.H. (1998) *J. Magn. Reson.*, **135**, 487–499.
- Goldman, M. (1984) *J. Magn. Reson.*, **60**, 437–452.
- Kloiber, K., Schuler, W. and Konrat R. (2002) *J. Biomol. NMR*, **22**, 349–363.
- McCoy, M.A. and Mueller, L. (1992) *J. Magn. Reson.*, Series A, **101**, 122–130.
- Palmer III, A.G., Skelton, N.J., Chazin, W.J., Wright, P.E. and Rance, M. (1992) *Mol. Phys.*, **75**, 699–711.
- Pelupessy, P., Espallargas, G.M. and Bodenhausen, G. (2003) *J. Magn. Reson.*, **161**, 258–264.
- Reif, B., Hennig, M. and Griesinger, C. (1997) *Science*, **276**, 1230–1233.
- Schwalbe, H. (2001) *Meth. Enzymol.*, **A338**, 35–81.
- Tjandra, N., Szabo, A. and Bax, A. (1996) *J. Am. Chem. Soc.*, **118**, 6986–6991.
- Yang, D., Konrat, R. and Kay, L. (1997) *J. Am. Chem. Soc.*, **119**, 11938–11940.